Astronomy & Astrophysics manuscript no. paper_printer_def ©ESO 2015
December 3, 2015

arXiv:1511.01425v2 [astro-ph.HE] 2 Dec 2015

The precessing jets of 1E 1740.7−2942

Pedro L. Luque-Escamilla[1,4], Josep Martí[2,4], and José Martínez-Aroza[3,4]

[1] Departamento de Ingeniería Mecánica y Minera, EPSJ, Universidad de Jaén, Campus Las Lagunillas s/n, A3-008, 23071 Jaén, Spain
e-mail: peter@ujaen.es

[2] Departamento de Física, EPSJ, Universidad de Jaén, Campus Las Lagunillas s/n, A3-420, 23071 Jaén, Spain
e-mail: jmarti@ujaen.es

[3] Departamento de Matemática Aplicada, Universidad de Granada, Campus de Fuente Nueva, 18071 Granada, Spain
e-mail: jmaroza@ugr.es

[4] Grupo de Investigación FQM-322, Universidad de Jaén, Campus Las Lagunillas s/n, A3-065, 23071 Jaén, Spain

Received Month xx, 2015; accepted Month xx, 2015

ABSTRACT

Context. The source 1E 1740.7−2942 is believed to be one of the two prototypical microquasars towards the Galactic center region whose X-ray states strongly resemble those of Cygnus X-1. Yet, the bipolar radio jets of 1E 1740.7−2942 are very reminiscent of a radio galaxy. The true nature of the object has thus remained an open question for nearly a quarter of a century.

Aims. Our main goal here is to confirm the Galactic membership of 1E 1740.7−2942 by searching for morphological changes of its extended radio jets in human timescales. This work was triggered as a result of recent positive detection of fast structural changes in the large-scale jets of the very similar source GRS 1758−258.

Methods. We carried out an in-depth exploration of the Very Large Array public archives and fully recalibrated all 1E 1740.7−2942 extended data sets in the C configuration of the array. We obtained and analyzed matching beam radio maps for five epochs, covering years 1992, 1993, 1994, 1997 and 2000, with an angular resolution of a few arcseconds.

Results. We clearly detected structural changes in the arc-minute jets of 1E 1740.7−2942 on timescales of roughly a year, which set a firm distance upper limit of 12 kpc. Moreover, a simple precessing twin-jet model was simultaneously fitted to the five observing epochs available. The observed changes in the jet flow are strongly suggestive of a precession period of ~ 1.3 years.

Conclusions. The fitting of the precession model to the data yields a distance of $\sim$ 5 kpc. This value, and the observed changes, rule out any remaining doubts about the 1E 1740.7−2942 Galactic nature. To our knowledge, this microquasar is the second whose jet precession ephemeris become available after SS433. This kind of information is relevant to the physics of compact objects, since the genesis of the precession phenomenon occurs very close to the interplay region between the accretion disk and the compact object in the system.

Key words. Stars: jets – ISM: jets and outflows – X-rays: binaries – Galaxies: jets – Stars: individual: 1E 1740.7−2942

1. Introduction

The microquasar 1E 1740.7−2942 was first detected with moderate signal-to-noise ratio during a Galactic plane survey conducted by the *Einstein X-ray Observatory* in soft X-rays (Hertz & Grindlay 1984). This object was later found to be the brightest hard-X source in the Galactic center region when observed by the coded aperture telescopes ART-P and SIGMA on board the Soviet GRANAT satellite (Sunyaev et al. 1991). The brightness of this object was rivaled only by that of the hard X-ray source GRS 1758−258 discovered by GRANAT a few degrees away from it. As a result of follow-up monitoring with SIGMA, 1E 1740.7−2942 attracted much attention when it was suggested to be a variable emitter of 511 keV e^-e^+ annihilation line (Bouchet et al. 1991). This finding was the origin of the "Great Annihilator" nickname for this microquasar.

The source 1E 1740.7−2942 made further headlines when it was proposed as a highly-absorbed microquasar in the Galactic center vicinity after the detection of bipolar radio jets emanating from it (Mirabel et al. 1992). Only a few months later, GRS 1758−258 was also shown to reveal the same radio jet morphology (Rodríguez et al. 1992), and thus both sources started to be considered sort of microquasar twins in the Galactic center region. Nevertheless, the absence of their respective optical or infrared counterparts precluded confirming their true Galactic nature via classical spectroscopic techniques. The main evidence supporting the microquasar interpretation was the extraordinary resemblance of X-ray spectral properties with those of the well-known black hole candidate Cygnus X-1 (see, e.g., Main et al. 1999). In this context, the presence of radio jets could also be interpreted as having been produced in ordinary radio galaxies. Alternatively, assuming a Galactic center distance of 8.5 kpc, the arc-minute angular dimensions of the radio jets translated into a parsec scale linear size of the collimated jet flows.

In contemporary times, the infrared counterpart of GRS 1758−258 has been confidently identified as a variable, point-like source whose spectral energy distribution agrees with a microquasar system harboring a low-mass stellar companion (Luque-Escamilla et al. 2014). For 1E 1740.7−2942, only a candidate counterpart has been reported in the near-infrared based on astrometric coincidence with the X-ray and radio position of the microquasar central core (Martí et al. 2010). Accounting for the high interstellar absorption towards this source, the observed magnitudes agree

with a high-mass X-ray binary (HMXB) or a low-mass X-ray binary (LMXB) microquasar, depending on the near-infrared emission being dominated or not by stellar emission and, of course, the assumed distance. Nevertheless, the apparently extended aspect of the infrared counterpart candidate still cast some doubts about the true Galactic origin of 1E 1740.7−2942 in case the extension was real and not due to crowding in the stellar field.

Very recently, GRS 1758−258 has been finally shown to be within the boundaries of the Milky Way. This statement is based on causality arguments applied to the discovery of major structural variations in its relativistic jets and lobes (Martí et al. 2015). The observed changes developed on timescales of about a decade, likely as a result of hydrodynamical instabilites. This finding prompted us to search for a similar behavior in 1E 1740.7−2942, which could also rule out the possibility of dealing with an extragalactic source. Although we have not detected evidence of major disruptive events in the Great Annihilator jet flow, noticeably morphological changes in its bipolar jets are certainly observed. An interpretation based on jet precession is tentatively proposed. In any case, the findings reported here confirm the marginal evidence for time variations in the 1E 1740.7−2942 extended jets historically reported by Mirabel & Rodríguez (1994b), and positively settle, at last, the issue of its Milky Way membership.

In Fig. 1 we provide a general view of the 1E 1740.7−2942 field for illustrative purposes. This figure shows the microquasar location in a complex region rich in extended radio emission from the Galactic plane. The central core of the system lies at the J2000.0 position $\alpha = 17^h43^m54\overset{s}{.}83$ and $\delta = -29°44'42\overset{''}{.}9$ (Martí et al. 2010). Other large-scale filamentary features, such as G359.10−00.20 also known as the Galactic center Snake (Yusef-Zadeh et al. 1984) are present as well. 1E 1740.7−2942 is actually located less than one degree away from Sagittarius A, at an angular distance equivalent to about five 6 cm primary beams of the Very Large Array (VLA) antennae.

2. Observations and data analysis

We carried out data mining at the public archives of the VLA hosted by the National Radio Astronomy Observatory (NRAO) in the US. The 1E 1740.7−2942 radio jets are well sampled with an angular resolution of a few arcseconds with the $\lambda = 6$ cm wavelength in the C configuration of the array. We thus searched for suitable VLA data sets with this instrumental setup and a reasonable integration time to produce a series of high-fidelity and sensitive maps with the same angular resolution. Having a good match of the map point spread function, or synthesized beam, is a mandatory condition for a meaningful comparison of the radio jet structural changes across different epochs. In Table 1, we list the VLA projects that we finally selected for our study.

Absolute flux density was based on the VLA primary amplitude calibrators 1331+305 and 0137+331, while the phase calibrator observed was always 1751−253. Most of the original observations were obtained using the old B1950.0 reference system. They were transformed into the current standard J2000.0 reference system with the AIPS task UVFIX.

Table 1. Log of VLA 6 cm observations used in this work.

Project Id.	Array Conf.	Observation Date	On-Source Time (s)	Central JD
AM345	C	1992 Mar 21	5280	
		1992 Apr 09	13410	2448719
		1992 Apr 11	5130	
AM415	C	1993 Aug 24	8180	
		1993 Aug 27	8150	2449226
		1993 Aug 28	8160	
AM453	C	1994 Dec 13	11260	2449707
		1994 Dec 27	12690	
AM565	C	1997 Jul 25	15070	2450657
		1997 Jul 28	16850	
AL511	C	2000 Apr 07	4490	2451642

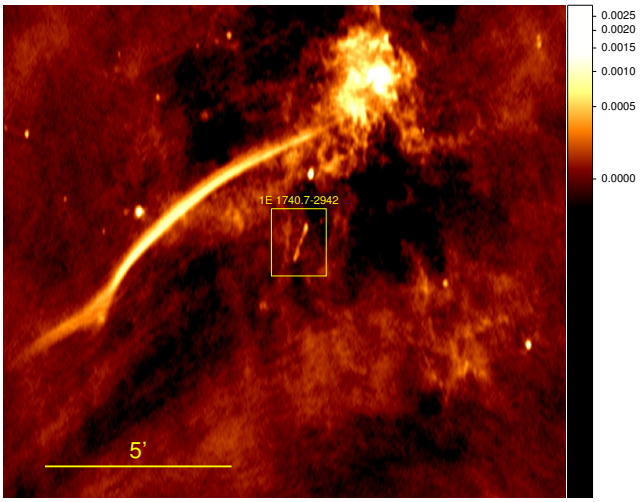

Fig. 1. Wide-field, deep VLA radio image of 1E 1740.7−2942 at the 6 cm wavelength obtained after combining all the visibility data listed in Table 1. The corresponding synthesized beam was $8\farcs16 \times 3\farcs47$, with position angle of $-1\fdg2$. The yellow box outlines the region occupied by the microquasar jets that we study with further detail in the rest of this work, while the long filamentary structure is the famous Galactic center Snake (Yusef-Zadeh et al. 1984). The horizontal yellow bar gives the angular scale. The total integration time amounts to 30 h. The resulting rms noise in this highly confused area of the Galactic center is estimated as 20 μJy beam^{-1}. Brightness level in a logarithmic scale is given by the color vertical bar in Jy beam^{-1}. North is up and east is left.

All raw data sets were retrieved and carefully recalibrated using the latest version of the AIPS software package of NRAO. Deconvolution of the dirty maps was based on the CLEAN algorithm, as provided by the AIPS task IMAGR. Weighting of the visibilities was pure natural (i.e., with a +5 value of the ROBUST parameter in the IMAGR task of AIPS) to better enhance sensitivity to the jet arc-minute emission. We also limited the baseline length to larger than 10 kλ to avoid confusion with the Galactic plane emission on much larger angular scales. Figure 2 shows the final result of our multiepoch analysis. The same average restoring beam has been used in all observing epochs.

3. Discussion

Figure 2 clearly shows that 1E 1740.7−2942 jets underwent obvious structural changes in a timescale of years. Subtraction of one panel from another (see Fig. 3 in the main text and Fig. 5 in the online material) provided strong residuals well above the root-mean-square (rms) noise by a factor

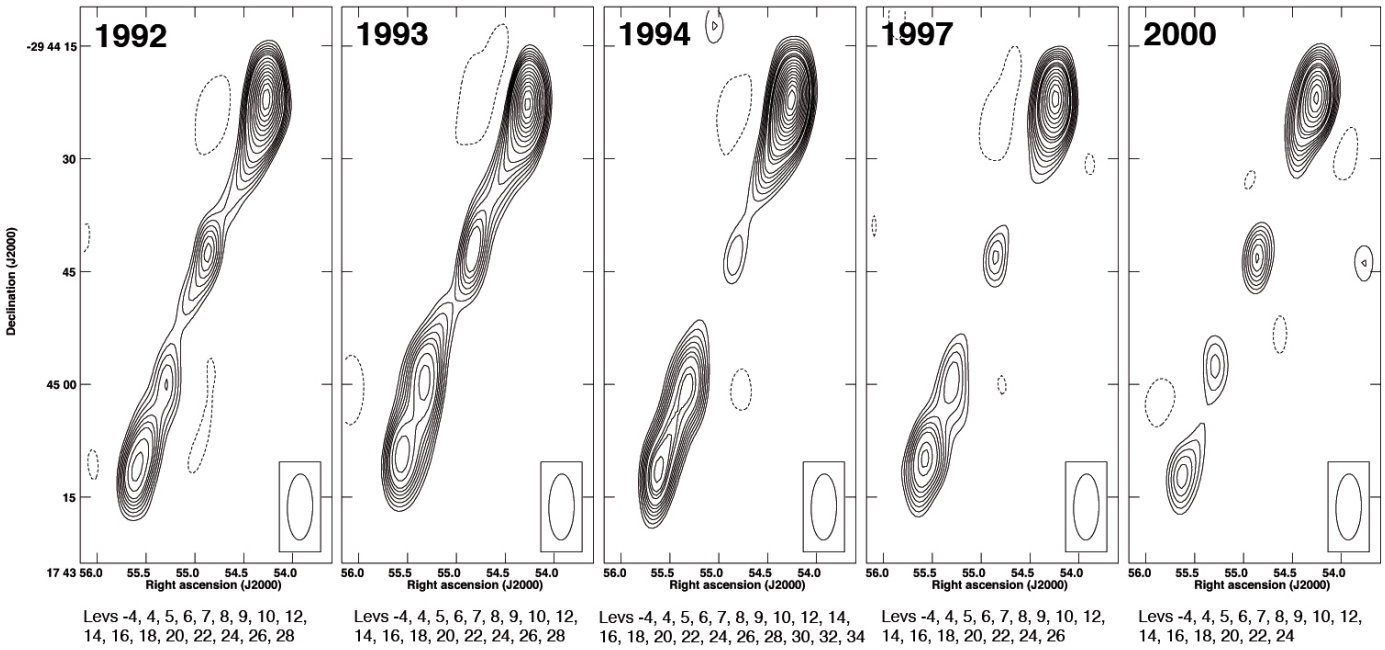

Fig. 2. Matching beam contour plots of the 1E 1740.7−2942 extended radio jets as observed with the VLA interferometer at the 6 cm wavelength (4.8 GHz) over the years 1992 to 1997. The respective rms background noise is 20.2, 19.1, 19.1, 21.6, and 21.5 μJy beam^{-1}. Contour levels in units of rms are given below each frame. The synthesized beam, with a size of $8\farcs78 \times 3\farcs38$ and $-0\fdg99$ position angle, is shown as an ellipse at the bottom right corner on each frame. North is up and east is left.

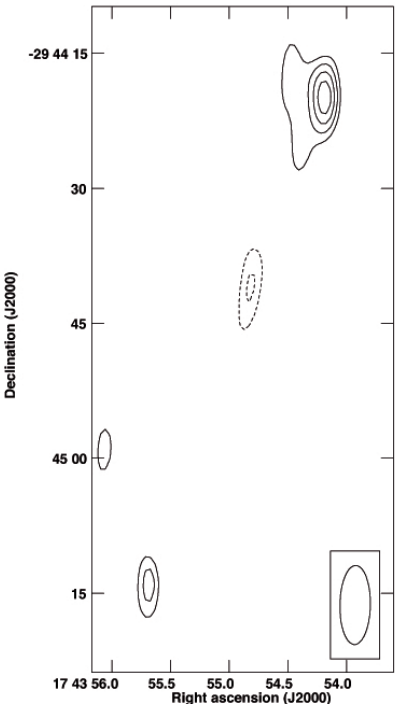

Fig. 3. One of the six maps of residuals obtained from the differences of the epochs shown in Fig 2. This one corresponds to the difference between the 1993 and the 1994 epochs. The rest of residual maps may be seen in the online data. Contour levels are −5, −3, 0, 2, 4, 6 times the rms noise, which amounts 28 μJy.

up to 6, thus adding confidence to the reality of the observed variations. This is further reinforced as we have independently obtained a residual map for the difference between 1993 − 1992, which is highly compatible with the historical analysis by Mirabel & Rodríguez (1994b). These authors

already anticipated the possibility of morphological changes in the 1E 1740.7−2942 radio lobes, although with less significance than in this work.

3.1. Distance upper limit

The most important consequence of the observed changes is an upper limit to the 1E 1740.7−2942 distance. This comes from the timescale ($\tau \simeq 1.3$ yr) of major structural changes in the bipolar lobes, especially between the 1994 and 1993 observations. The deconvolved angular size of the strongest northern lobe is about $\theta \simeq 7''$. This representative value comes from an elliptical Gaussian fit using the AIPS task JMFIT on the Fig. 2 maps, and averaging the major axis over all epochs. Hence, causality arguments dictate that the maximum possible distance lies within the boundaries of the Milky Way ($\sim c\tau/\theta \sim 12$ kpc). Therefore, we can now be sure that 1E 1740.7−2942 joins the family of Galactic microquasars just as its twin GRS 1758−258.

3.2. Evidences of precession

However, the time evolution of the extended radio jets of 1E 1740.7−2942 does not seem to respond to the same physical arguments based on hydrodynamical instabilities invoked in the GRS 1758−258 case (Martí et al. 2015). For 1E 1740.7−2942, the morphology changes shown in Fig. 2 are instead strongly reminiscent of the precessing radio jets of the well-known microquasar SS433 (Hjellming & Johnston 1981). It is appropriate to mention here that hints of precession in 1E 1740.7−2942 have been previously reported based on X-ray data analysis (del Santo et al. 2005).

3.2.1. A straight line jet?

Before seriously adopting a precession scenario, one should consider whether the wavy appearance of the jets could arise from individual point-like blobs moving along a straight path, and observed with the poor resolution of the synthesized beam in the north-south direction. Including the core, at least four of these blob maxima are well visible in each Fig. 2 contour plot. In order to test the quality of a linear fit forced to pass through the central core, we use a reduced χ^2 approach as follows. Let $N_{\rm p}$ be the total number of positions along the jet measured with respect to the microquasar central core position. At each point with angular coordinates $[\Delta\alpha_i \cos\delta, \Delta\delta_i]$ ($i = 1, ..., N_{\rm p}$), we assign uncertainties $[\sigma_{\alpha_i}, \sigma_{\delta_i}]$ given by the synthesized beam size divided by the local signal-to-noise ratio of the jet radio emission. Each point has two differential coordinates, thus the total number of observables to be fitted is $2N_{\rm p}$ (in this case $2N_{\rm p} = 8$). The reduced χ^2 function is defined as

$$\chi^2_{\rm red} \equiv \frac{\Sigma_{i=1}^{i=N_{\rm p}} \left\{ \left[\frac{\Delta\alpha_i - \Delta\alpha_{\rm fit}}{\sigma_{\alpha_i}} \right]^2 \cos^2\delta + \left[\frac{\Delta\delta_i - \Delta\delta_{\rm fit}}{\sigma_{\delta_i}} \right]^2 \right\}}{2N_{\rm p} - N_{\rm par}}, \quad (1)$$

where $[\Delta\alpha_{\rm fit}\cos\delta, \Delta\delta_{\rm fit}]$ are the expected jet differential coordinates at each point from a fitting model with $N_{\rm par}$ parameters ($N_{\rm par} = 1$ for the slope of the straight line). A fit with $\chi^2 \lesssim 1$ is considered very acceptable.

The four condensations quoted above turn out not to be well aligned in all epochs. This is better illustrated in online Fig. 6, where the fit is particularly bad, with $\chi^2_{\rm red} = 4.4$. This could suggest a curved jet with some component of blob motion perpendicular to the jet axis, which points again to precession. Moreover, we also tried to check the assumed compact nature of the blobs by subtracting a point-like source model at each of their positions. Full removal of their emission was not possible unless an extended Gaussian model was used. Therefore, the 1E 1740.7−2942 jet structure seems more likely to consist of a continuous, extended, and precessing jet instead of individual, compact blobs all moving along the same straight path.

3.2.2. Fitting a precessing jet

To provide additional support to the precession hypothesis, we carried out another series of fits to the projected jet paths of 1E 1740.7−2942. The jet loci were more carefully estimated from the Fig. 2 maps with two different methods. First, by slicing the jet in the north-south direction pixel by pixel and keeping the location of maxima in the jet profiles, we estimated position uncertainties as in the previous section and we only kept jet points with signal-to-noise ratio above 5. Second, extracting the jet skeleton using the mathematical morphology approach (Serra & Cressie 1982), allowed us to build two independent estimates of the jet path, or jet skeletons, whose differences are always less than a small fraction of the synthesized beam. To fit these data, we carried out a SS433-like fit with the same kinematic model developed by Hjellming & Johnston (1981) several decades ago ($N_{\rm par} = 7$). In contrast to this classical case, here we do not have any additional information from radial velocity changes in the jet flow. The historical 511 keV emission line feature attributed to 1E 1740.7−2942, if really originating in the jets, was too broad and too sparsely sampled to assist us in the fit from the Doppler point of view. Therefore, to our knowledge this is the first time that a multiepoch fit of a relativistic twin-jet kinematic model is attempted based only on the changing jet path projected onto the celestial sphere. For comparison purposes, we also fitted a straight line passing through the system's central core ($N_{\rm par} = 1$ for each epoch). In both cases, a single $\chi^2_{\rm red}$ value is computed via Eq. 3.2.1, but now with $N_{\rm p} \sim 500$. It is important to stress here that all jet paths, on the five different epochs, were simultaneously fitted with the same set of model parameters.

The model fits to the jet maxima skeleton are presented in online Fig. 7. Again, the simple straight line model does not provide a good description of the data. Typically, one obtains $\chi^2_{\rm red} \gtrsim 2$. The same is true when fitting the mathematical morphology skeletons. On the other hand, significantly better fits are possible when using the precessing jet model. After exploring a reasonable range of values in the parameter space, including the distance, we obtained the best fit with the jet maxima skeleton with $\chi^2_{\rm red} = 0.91$. This was followed by the $\chi^2_{\rm red} = 1.26$ value provided by

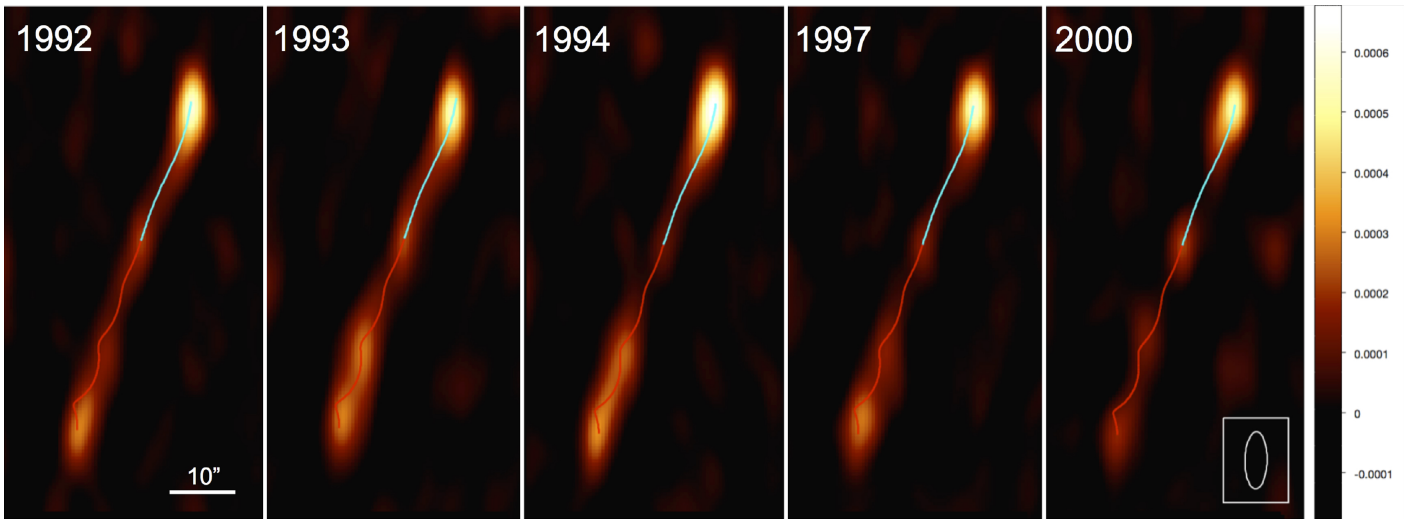

Fig. 4. Fit of a precessing twin jet model (red receding; blue approaching) using the Table 2 parameters based on the mathematical morphology skeleton that yields $\chi^2_{\rm red} = 1.26$. The fit is overlayed onto false-color maps of the 1992, 1993, 1994, 1997, and 2000 VLA data sets. The horizontal bar gives the angular scale in arcseconds, and the vertical bar illustrates the brightness scale in Jy beam^{-1}. The restoring beam used is shown at the bottom right corner. North is up and east is left.

the mathematical skeleton approach, which is also shown in Fig. 4. Their respective seven parameters are given in Table 2. A comparison of these parameters does not reveal differences that are too large. Varying these parameters by no more than 10% still provides an acceptable agreement, except for the inclination of the jet precession axis (±5%) and the inclination of the approaching jet axis to north (±1%).

The remarkable good match between the observed jets and the fitted models suggests that the dominant effect determining the extended structure of the 1E 1740.7−2942 radio jets is very likely due to precession.

3.2.3. Implications of the precession model

Our analysis has to be considered as an exploratory but instructive exercise while waiting for additional epochs to be obtained. Although precession appears to be well established, caution is still advisable about its true period because the range of precession phases currently sampled by available data is still very small ($\sim$ 10% of precession cycle). The suggested 5 kpc distance to 1E 1740.7−2942, if correct, comes as a striking result, and not only because of its consistent agreement with the upper limit derived above. This value would put 1E 1740.7−2942 much closer than usually agreed. Forcing the distance to remain inside the range 8-12 kpc our best fit was obtained for 8 kpc, but it was not very good ($\chi^2_{\rm red} = 1.23$ using maxima skeleton). The rest of fitted parameters did not change significantly, except for a slightly less relativistic jet velocity ($v_{\rm jet} = 0.75c$) and a higher inclination. In this case, it is remarkable that the preferred inclination was > 90°, thus implying that the fainter southern jet would be the approaching one. The fits also appeared visually too wavy in the northern jet, in contrast to the observed smoother jet paths in Fig. 2.

In the absence of further observational data, we adopt the lowest χ^2 solution as the most likely to proceed our discussion. At 5 kpc, the arc-minute extension of the jets would then span to a

Table 2. Twin-jet kinematic model for 1E 1740.7−2942 radio jets(*)

Parameter	Mathematical morphology skeleton	Maxima skeleton
Angle of the precession cone	$\psi = 1\overset{\circ}{.}8$	$\psi = 2\overset{\circ}{.}3$
Inclination of the jet precession axis with the l.o.s.	$i = 65\overset{\circ}{.}1$	$i = 63\overset{\circ}{.}0$
Position angle of the jet precession axis	$\chi = 339\overset{\circ}{.}6$	$\chi = 338\overset{\circ}{.}5$
Precession period	$P_{\rm p} = 481.8$ d	$P_{\rm p} = 485.5$ d
Reference JD(**)	$t_{\rm ref} = 2448303.51$	$t_{\rm ref} = 2448307.85$
Jet velocity	$v_{\rm jet} = 0.96c$	$v_{\rm jet} = 0.88c$
Distance	$d = 5$ kpc	$d = 5$ kpc
Approaching jet (N)	$s_{\rm jet} = +1$ (fixed)	$s_{\rm jet} = +1$ (fixed)
Receding jet (S)	$s_{\rm jet} = -1$ (fixed)	$s_{\rm jet} = -1$ (fixed)
Sense of rotation (counterclockwise)	$s_{\rm rot} = +1$ (fixed)	$s_{\rm rot} = +1$ (fixed)
Goodness of fit	$\chi^2_{\rm red} = 1.26$	$\chi^2_{\rm red} = 0.91$

(*) Adapted from Hjellming & Johnston (1981).
(**) Corresponding to zero precession phase.

length of 1.5 pc. This newly proposed distance is not strictly precluded in any of the analysis up to now, and is in agreement with the arguments already pointed out by Mereghetti et al. (1992). Only some concern could emerge about the possible conflict with the extremely high column density ($N_{\rm H} = 1.2 \times 10^{23}$ cm^{-2}) attributed to 1E 1740.7−2942 from X-ray spectral fits (Gallo & Fender 2002). However, one cannot rule out that an intrinsic source of extinction, such as a slow and dense stellar wind, is at work.

The newly proposed distance implies consequences for some of the estimations made for the 1E 1740.7−2942 system in previous works. In particular, the absolute magnitude of the infrared counterpart candidate proposed in Martí et al. (2010) should be revised to $K_s = -3.0$. At 5 kpc, this would be consistent with an early-type B star on the main sequence or a middle-KIII giant star. This last option is especially interesting because it would render 1E 1740.7−2942 a system similar to the superluminal microquasar GRS 1915+105, hosting a similar giant companion star (Greiner et al. 2001). A more common LMXB scenario, with a much fainter nondegenerate companion star, still remains conceivable if the near-infrared luminosity arises from the ensemble of an accretion disk plus jet, as in GRS 1758−258. A better knowledge of the system spectral energy distribution is required to discriminate among all these options.

The jet in 1E 1740.7−2942 seems to be highly collimated, with a small precession cone angle of few degrees, and a precession period $P_{\rm p} \simeq 1.3$ yr. Smith et al. (2002) found two super-orbital periods for 1E 1740.7−2942 , the main period of $\sim$ 600 d, and the other of $\sim$ 490 d (or 1.34 yr). Given their remarkable proximity, it is very tempting to associate this second super-orbital period with the precession cycle proposed here.

Larwood (1998) derived a theoretical relation between orbital and precession periods in X-ray binary systems. Assuming a system with small orbital inclination and mass ratio between star and compact object in the range μ = 0.2-20, the precession to orbital period ratio is predicted to be in the range $P_{\rm p}/P \sim$ 18-40. From our precession period, and the orbital period P = 12.7 d obtained by Smith et al. (2002), this ratio becomes about 37 in our case. This value would point to a mass ratio close to $\sim$ 0.2. Let us further consider plausible values of a $\sim 1 M_{\odot}$ mass for the companion and $\sim 5 M_{\odot}$ mass for the black hole compact object. The semimajor axis of the orbit would then be $\sim$ 0.36 AU, while the Roche lobe radius would amount $\sim$ 25% of this value (Eggleton 1983). Under these kinds of assumptions, the 1E 1740.7−2942 companion would need to be a giant star to fill such a Roche lobe. This would be in agreement with the dereddened absolute magnitude quoted above consistent with a KIII star. Alternatively, in the case of a B-type companion, the mass transfer should most likely proceed via the stellar wind.

Bulk jet flow velocities close to the speed of light c have been inferred in several X-ray binaries such as GRS 1915+105 (Mirabel & Rodríguez 1994a). Thus, the high values of $v_{\rm jet}$ obtained here for 1E 1740.7−2942 do not come as a surprise. The only relevant aspect is that our fits suggest that the jet flow remains ballistic and highly relativistic until decelerated very close to the hotspots. From standard equipartition arguments applied to the VLA maps, the total energy content in the lobes is estimated to be $\sim 5 \times 10^{43}$ erg with a magnetic field $B \sim 10^{-4}$ G. Assuming steady, continuous, ballistic jets, the obtained velocity allows us to estimate that the radio lobe particle content is renewed on a timescale of $\sim 10^3$ d, i.e., the jet travel time. The corresponding total energy output from the central core is then estimated to be $\sim 10^{36}$ erg s^{-1}. This number is of the same order as in SS433 (Hjellming & Johnston 1981) and slightly less than estimated in the Cygnus X-3 case (Sánchez-Sutil et al. 2008).

4. Conclusions

An in-depth reanalysis of selected data sets of 1E 1740.7−2942 in the NRAO archive in the time interval 1992-2000 has been presented that sheds new light on the nature of this bipolar jet source. Clear morphological variability has been detected in the arc-minute extended radio jet on yearlong timescales that confirm the suspicions in this sense advanced two decades ago by Mirabel & Rodríguez (1994b). Difference maps between observing epochs provide very significative residuals, and this evidence changes in the system radio lobes with a high level of confidence (up to 6σ). This fact clearly rules out an extragalactic origin for 1E 1740.7−2942 and ensures its Galactic microquasar nature. Moreover, from simple causality arguments a safe 12 kpc upper limit to its distance is derived.

In addition, the 1E 1740.7−2942 jets show a changing wavy appearance from epoch to epoch that is very suggestive of precession. We tentatively fitted a precessing twin-jet model that surprisingly yielded very promising results. A single set of jet parameters simultaneously reproduces the

observed jet paths in all five observing epochs. The source 1E 1740.7−2942 thus becomes the second microquasar after SS433 for which an ephemeris of its precessing relativistic jets is foreseen.

Our preliminary exploration of the parameter space in the precession model favors a distance of about 5 kpc, i.e., significantly closer than the Galactic center and consistent with the previous upper limit. In addition, the precession period of 1.33 yr provided by our fit is practically coincident with one of the super-orbital period reported by Smith et al. (2002) based on X-ray data analysis.

The closer distance, and also the ratio between the precession and orbital period, are found to be reasonably consistent with 1E 1740.7−2942, which is a LMXB microquasar system harboring a giant late-type giant companion filling its Roche lobe. Nevertheless, the currently available data does not strictly rule out a HMXB alternative scenario with a main-sequence B-type star.

We did not need to account for any jet deceleration when fitting the data, thus suggesting that the jet flow remains highly relativistic until very close to the terminal hotspots. The corresponding timescales for renewal of the energy content in the 1E 1740.7−2942 radio lobes imply that the central engine is able to inject $\sim 10^{36}$ erg s^{-1} into the relativistic jet flow. This value compares satisfactorily with other Galactic microquasars such as SS433 and Cygnus X-3.

Future interferometric observations of 1E 1740.7−2942 over the years will allow a more accurate follow-up of the time evolution of its bipolar radio jets, and consequently enable a really robust fit to the jet kinematical parameters.

Acknowledgements. The National Radio Astronomy Observatory is a facility of the National Science Foundation operated under cooperative agreement by Associated Universities, Inc. Authors acknowledge support by grant AYA2013-47447-C3-3-P from the Spanish Ministerio de Economía y Competitividad (MINECO), and by Consejería de Economía, Innovación, Ciencia y Empleo of Junta de Andalucía under excellence grant FQM-1343 and research group FQM-322, as well as FEDER funds.

References

Bouchet, L., Mandrou, P., Roques, J. P., et al. 1991, ApJ, 383, L45

del Santo, M., Bazzano, A., Zdziarski, A. A., et al. 2005, A&A, 433, 613

Eggleton, P. P. 1983, ApJ, 268, 368

Gallo, E. & Fender, R. P. 2002, MNRAS, 337, 869

Greiner, J., Cuby, J. G., McCaughrean, M. J., Castro-Tirado, A. J., & Mennickent, R. E. 2001, A&A, 373, L37

Hertz, P. & Grindlay, J. E. 1984, ApJ, 278, 137

Hjellming, R. M. & Johnston, K. J. 1981, ApJ, 246, L141

Larwood, J. 1998, MNRAS, 299, L32

Luque-Escamilla, P. L., Martí, J., & Muñoz-Arjonilla, Á. J. 2014, ApJ, 797, L1

Main, D. S., Smith, D. M., Heindl, W. A., et al. 1999, ApJ, 525, 901

Martí, J., Luque-Escamilla, P. L., Romero, G. E., Sánchez-Sutil, J. R., & Muñoz-Arjonilla, Á. J. 2015, A&A, 578, L11

Martí, J., Luque-Escamilla, P. L., Sánchez-Sutil, J. R., et al. 2010, ApJ, 721, L126

Mereghetti, S., Caraveo, P., Bignami, G. F., & Belloni, T. 1992, A&A, 259, 205

Mirabel, I. F. & Rodríguez, L. F. 1994a, Nature, 371, 46

Mirabel, I. F. & Rodríguez, L. F. 1994b, in American Institute of Physics Conference Series, Vol. 304, American Institute of Physics Conference Series, ed. C. E. Fichtel, N. Gehrels, & J. P. Norris, 413–420

Mirabel, I. F., Rodríguez, L. F., Cordier, B., Paul, J., & Lebrun, F. 1992, Nature, 358, 215

Rodríguez, L. F., Mirabel, I. F., & Martí, J. 1992, ApJ, 401, L15

Sánchez-Sutil, J. R., Martí, J., Combi, J. A., et al. 2008, A&A, 479, 523

Serra, J. & Cressie, Noel A. C, C. 1982, Image analysis and mathematical morphology (London, Orlando, New York: Academic press), autres tirages : 1984, 1988 (avec corrections), 1989, 1990, 1993

Smith, D. M., Heindl, W. A., & Swank, J. H. 2002, The Astrophysical Journal Letters, 578, L129

Sunyaev, R., Churazov, E., Gilfanov, M., et al. 1991, A&A, 247, L29

Yusef-Zadeh, F., Morris, M., & Chance, D. 1984, Nature, 310, 557

List of Objects

‘1E 1740.7−2942’ on page 1

‘1E 1740.7−2942’ on page 1

‘Cygnus X-1’ on page 1

‘1E 1740.7−2942’ on page 1

‘1E 1740.7−2942’ on page 1

‘GRS 1758−258’ on page 1

‘1E 1740.7−2942’ on page 1

‘1E 1740.7−2942’ on page 1

‘1E 1740.7−2942’ on page 2

‘SS433’ on page 2

‘1E 1740.7−2942’ on page 2

‘GRS 1758−258’ on page 2

‘1E 1740.7−2942’ on page 2

‘1E 1740.7−2942’ on page 2

‘GRS 1758−258’ on page 2

‘Cygnus X-1’ on page 2

‘GRS 1758−258’ on page 2

‘1E 1740.7−2942,’ on page 2

‘1E 1740.7−2942’ on page 3

‘GRS 1758−258’ on page 3

‘1E 1740.7−2942,’ on page 3

‘1E 1740.7−2942’ on page 3

‘1E 1740.7−2942’ on page 3

‘1E 1740.7−2942’ on page 3

‘1E 1740.7−2942’ on page 3

‘1331+305’ on page 3

‘0137+331’ on page 3

‘1751−253’ on page 3

‘1E 1740.7−2942’ on page 4

‘1E 1740.7−2942’ on page 4

‘1E 1740.7−2942’ on page 5

‘1E 1740.7−2942’ on page 6

‘1E 1740.7−2942’ on page 6

‘1E 1740.7−2942’ on page 6

‘GRS 1758−258’ on page 6

‘1E 1740.7−2942’ on page 6

‘GRS 1758−258’ on page 6

‘1E 1740.7−2942’ on page 6

‘SS433’ on page 6

‘1E 1740.7−2942’ on page 6

‘1E 1740.7−2942’ on page 7

‘1E 1740.7−2942’ on page 7

‘SS433’ on page 7

‘1E 1740.7−2942’ on page 7

‘1E 1740.7−2942’ on page 8

‘1E 1740.7−2942’ on page 8

‘1E 1740.7−2942’ on page 8

‘1E 1740.7−2942’ on page 9

‘1E 1740.7−2942’ on page 9

‘1E 1740.7−2942’ on page 9

‘1E 1740.7−2942’ on page 9

‘GRS 1758−258’ on page 9

‘1E 1740.7−2942’ on page 9

‘1E 1740.7−2942’ on page 9

‘1E 1740.7−2942’ on page 10

‘1E 1740.7−2942’ on page 10

‘SS433’ on page 10

‘Cygnus X-3’ on page 10

‘1E 1740.7−2942’ on page 10

‘1E 1740.7−2942’ on page 10

‘1E 1740.7−2942’ on page 10

‘The source 1E 1740.7−2942 thus’ on page 11

‘SS433’ on page 11

‘1E 1740.7−2942, which is’ on page 11

‘1E 1740.7−2942’ on page 11

‘SS433’ on page 11

‘Cygnus X-3’ on page 11

‘1E 1740.7−2942’ on page 11

‘1E 1740.7−2942’ on page 15

‘1E 1740.7−2942’ on page 16

‘1E 1740.7−2942’ on page 17

‘1E 1740.7−2942’ on page 17

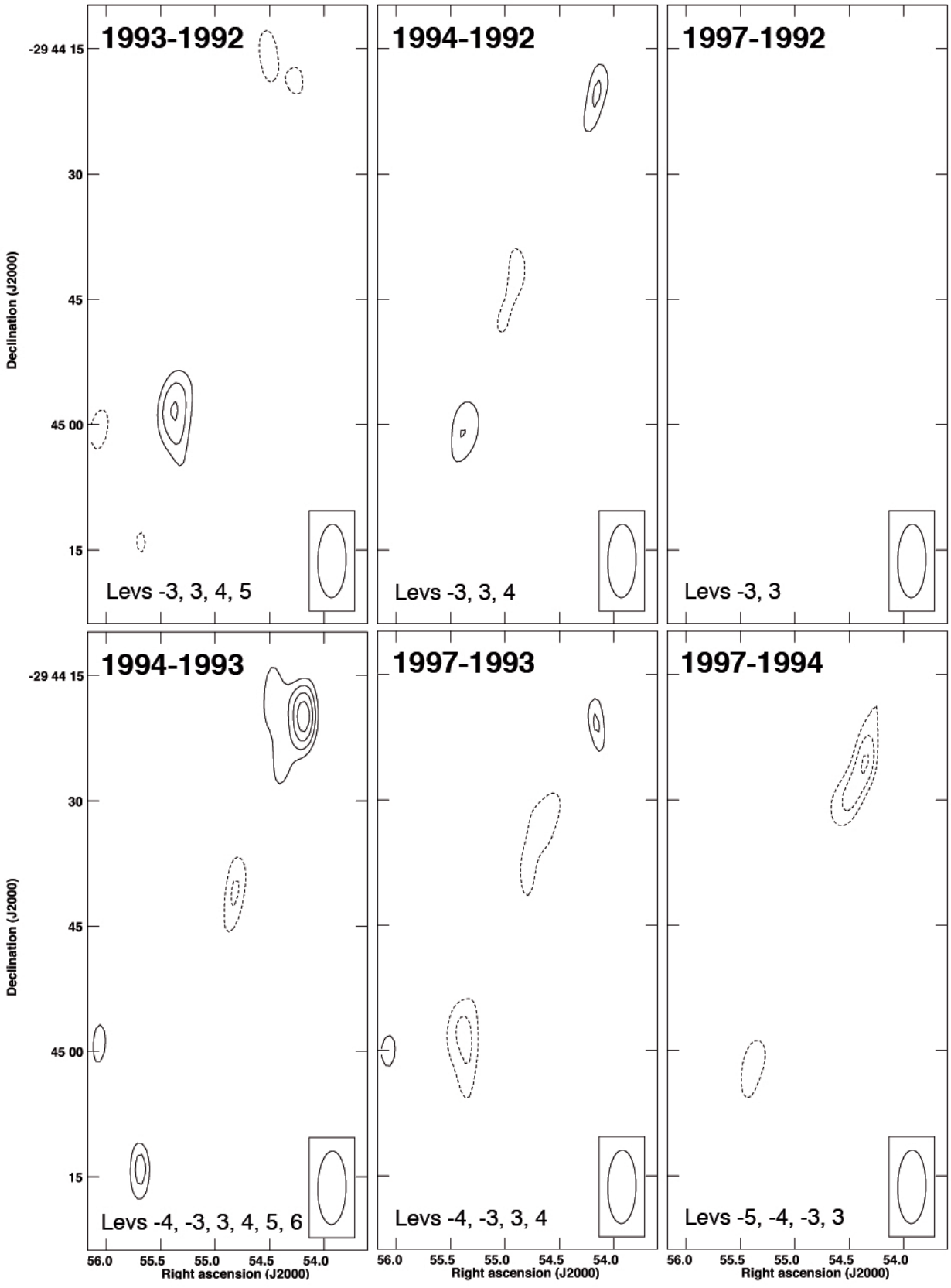

Fig. 5. Residuals obtained from the differences between the maps in Fig 2, as indicated on top of each frame. From left to right and up to down, the rms noise in μJy beam^{-1} is 28, 28, 29.6, 28, 29, and 29, respectively. Contour levels are given in units of rms noise at the bottom of each panel. All residuals tend to be well aligned with the jet position angle. The map corresponding to the 2000 epoch has not been used because 1E 1740.7−2942 was not at the phase center and the primary beam corrections would then render the difference maps meaningless.

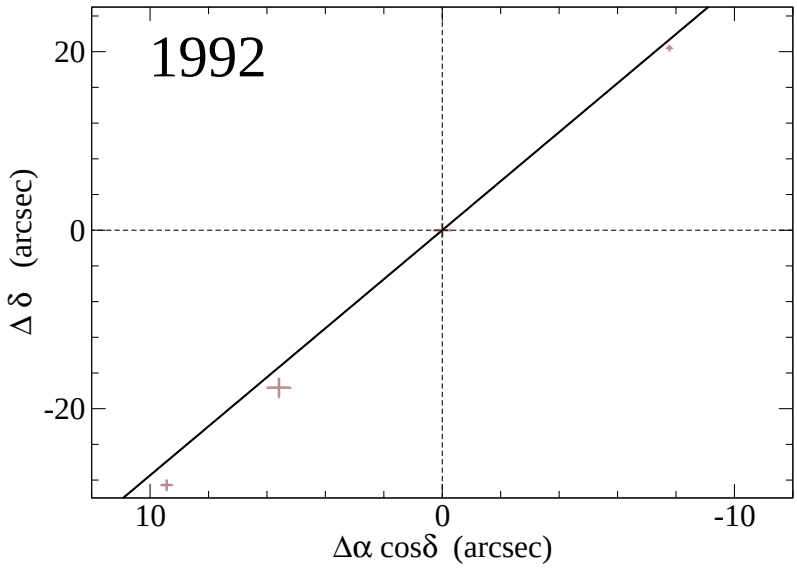

Fig. 6. Attempt to fit the 1992 location of the most prominent four condensations in the 1E 1740.7−2942 jet with a simple straight jet line model passing through the central core, which results in a rather poor 4.4 value of $\chi^2_{\rm red}$.

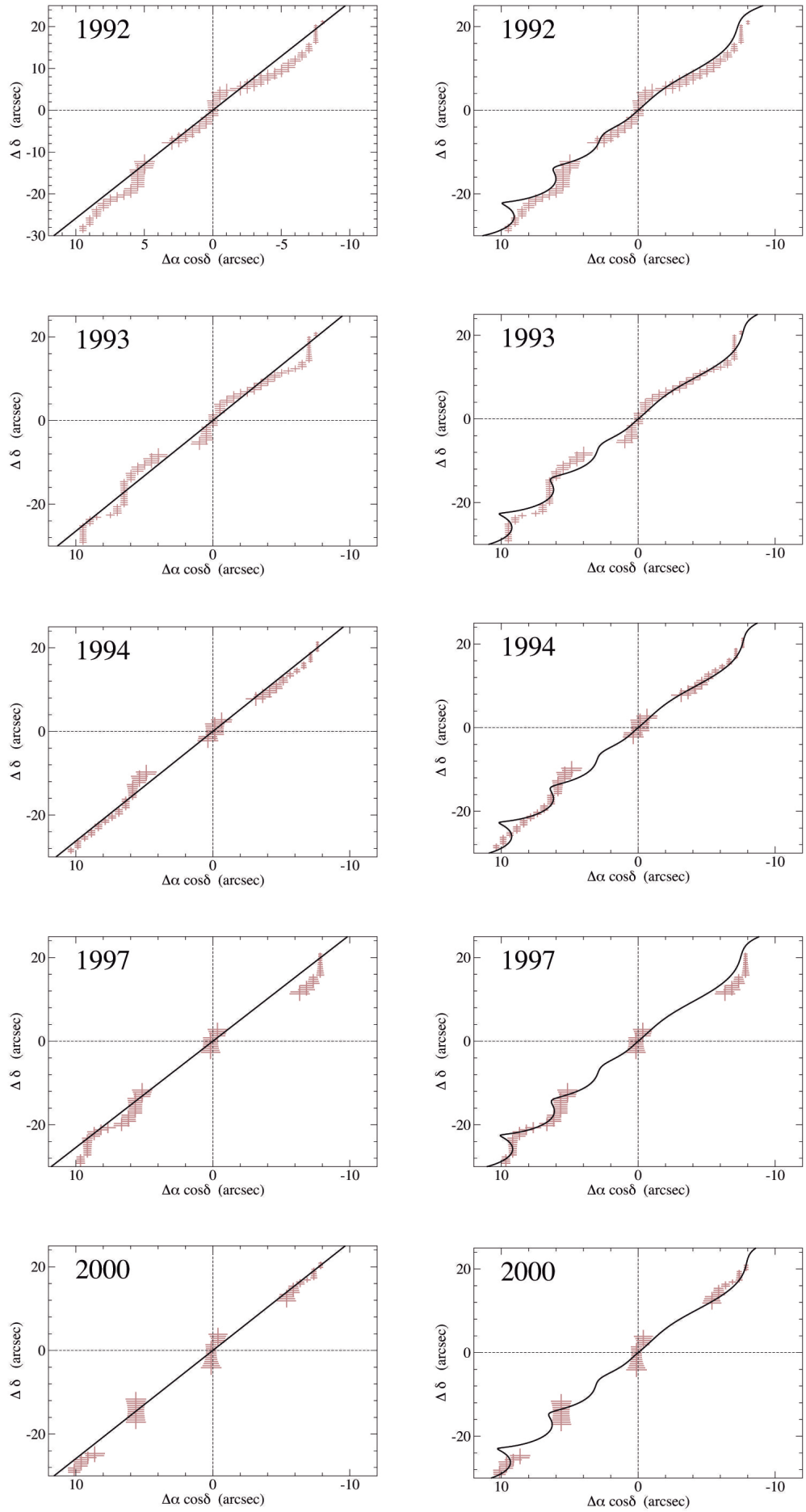

Fig. 7. Left. Attempts to fit the 1992 to 2000 observing epochs of the 1E 1740.7−2942 radio jets using rectilinear trajectories (thick lines). All of these emanate from the central core located at the intersection of the dashed lines. The brown crosses denote the observed jet path based on the maxima skeleton discussed in the text. The horizontal scale has been expanded to better show the straight line displacements from the jet flow. The reduced $\chi^2_{\rm red}$ value of the combined five epoch fit amounts to 2.2. **Right.** Fits to the 1992 to 2000 observing epochs of the 1E 1740.7−2942 radio jets based on the Hjellming & Johnston (1981) precessing twin jet model (thick lines). To facilitate an easy comparison, the outline of these plots is the same as in the left panel except for the fitting curves. We used the corresponding model parameter values given in right column of Table 2. The fit agreement with the observed jet paths appears to be significantly better here, with a reduced $\chi^2_{\rm red}$ value as low as 0.91.